A Proposed Technique to Acquire Cavity Pressure Using a Surface Strain Sensor During Injection-Compression Molding

Wei-Sheng Guan

Han-Xiong Huang[1]
e-mail: mmhuang@scut.edu.cn

Center for Polymer Processing Equipment and Intellectualization, The Key Laboratory of Polymer Processing Engineering of the Ministry of Education, South China University of Technology, Guangzhou 510640, PRC

A new technique was proposed and experimentally verified for the cavity pressure acquisition in the injection-compression molding (ICM). The surface strain of the fixed mold half and the cavity pressure were monitored simultaneously during ICM. In the compression stage, a directly proportional relationship between the cavity pressure and mold surface strain was found and determined via the regression analysis. By taking the advantage of this relationship, the cavity pressure profile with high accuracy was indirectly obtained from the nondestructive measurement of the mold surface strain. Moreover, the mold surface strain profile could indicate the part weight or thickness and the critical time when the part surface lost contact with the cavity surface in a large area. The monitoring of the mold surface strain could serve as an interesting alternative to the direct monitoring of the cavity pressure with respect to process and part quality control for ICM. [DOI: 10.1115/1.4023376]

Keywords: injection-compression molding, cavity pressure, online monitoring, surface strain

1 Introduction

During the injection molding, the polymeric material undergoes complicated thermomechanical history featuring obvious pressure variations as well as rapid cooling, and consequently experiences significant changes in its physical properties. As a result, the final quality of the molded part is inherently difficult to predict without sophisticated computer simulation software [1]. To achieve and maintain high quality of the molded parts, considerable researches have been reported on process monitoring and control of injection molding over the last two decades [2–9]. Among the process variables in injection molding, which mainly include melt pressure (in the nozzle [2,3], runner [2], and cavity [2–9]) and melt temperature (in the nozzle, runner [1], and cavity [2,7]), the cavity pressure is widely recognized to be especially critical to the process control and final part qualities. Specifically, the cavity pressure is found to be a reliable indicator for the shrinkage, warpage, weight, and thickness of the molded part.

ICM combing the injection molding with compression molding was developed to incorporate the advantages of both molding processes, including decreased molding pressure, shortened molding cycle, reduced part residual stress, and increased part dimensional accuracy [10–14]. It is a well-known technology to produce optical parts, such as diffraction grating [12], lens [13], and light guide [15] with tight tolerance and high optical performance. Despite the advantages associated with ICM, its process control is more critical and difficult since additional compression-related processing parameters are involved. The role of processing parameters playing in the part quality, which have been investigated experimentally [11,12,15–18] or numerically [10,11,14] in a wide range, is demonstrated to be significant. Moreover, in the complex process of ICM, the obvious changes in process variables (especially cavity pressure) can distinctly influence and also reflect the part quality. The cavity pressure in the compression stage, which experiences the most dramatic changes throughout the ICM process, is particularly necessary to be monitored for the process and part quality control, and thus has been placed special attention [10,11,14,19].

To implement the measurement of pressure, a variety of pressure sensors based on piezoelectric [2,9] and piezoresistive materials, load cells, strain gages [20], and optical fiber [21] have been developed. The wired piezoelectric pressure sensor is widely employed in the process monitoring and control during injection molding and extrusion. Because the injection mold usually contains complicated geometries, it is expensive to install wires through the mold to connect a sensor. To solve this problem, the wireless piezoelectric pressure sensor is developed recently [22,23]. Moreover, using the optical pressure sensor, the remote measurement of the displacement of a sensor diaphragm can be achieved, that is, the sensing electronics is remote from the working environment (e.g., mold cavity). This is quite beneficial for the miniaturization and robustness of sensor. Nevertheless, the cavity pressure measurement during injection molding generally requires the incorporation of a pressure sensor directly into the cavity, which makes this measurement difficult to be realized during molding optical and micro parts [24]. To the best knowledge of the authors, there are still few works on indirect monitoring techniques for the cavity pressure during ICM.

For the aforementioned reasons, a new technique was proposed to indirectly acquire the cavity pressure profile in the compression stage of ICM with the aid of the mold surface strain measurement in this work. The online monitoring of the mold surface strain and cavity pressure was carried out during ICM. In the compression stage, a quantitative relationship between the cavity pressure and mold surface strain was determined by the regression analysis. Applying this relationship, the cavity pressure with high accuracy could be obtained via the nondestructive monitoring of the mold surface strain. Moreover, some valuable information for the process and part quality control could also be acquired from the mold surface strain profile.

2 Experimental

2.1 Setup and Material. The ICM experiments were performed on an 80-ton injection-molding machine (KM80SP180CX, Krauss-Maffei). The injection-compression mold with a maximal

[1]Corresponding author.

Contributed by the Manufacturing Engineering Division of ASME for publication in the Journal of Manufacturing Science and Engineering. Manuscript received November 15, 2011; final manuscript received December 26, 2012; published online March 22, 2013. Assoc. Editor: Robert Gao.

compression stroke of 10 mm was used for molding the rectangular part with nominal dimensions of $120 \times 20 \times 2$ mm^3. The fixed mold half is schematically illustrated in Fig. 1.

A piezoelectric surface strain sensor (9232A, Kistler) was mounted on the external surface of the fixed mold half to monitor the mold strain in the horizontal direction during molding, as shown in Fig. 1. The strain of the mold leads to a change in distance between the two contact elements on the sensor. And the change in distance converts into a force acting on the piezoelectric materials, which produces an electric charge proportional to this force. Compared with the familiar wire strain gage, the piezoelectric surface strain sensor exhibits higher sensitivity and larger overload resistance. Piezoelectric pressure sensors (6190BA, Kistler) were mounted in two locations along the flow path, which are 40 and 120 mm from the sprue and denoted as P1 and P2, respectively (Fig. 1). The mold cavity corresponding to P1 is initially filled in the injection stage, whereas the mold cavity corresponding to P2 is filled in the subsequent compression stage. The upstream (P1) pressure was used to relate with the mold surface strain, and an indirect pressure acquisition technique was proposed based on the relationship developed. Knowing that the cavity pressure is consistently reduced along the flow path during ICM [10,19], comparing the downstream (P2) pressure with the upstream (P1) pressure can disclose the cavity pressure uniformity. For each molding cycle investigated, online data were collected simultaneously from the three sensors using a data acquisition system (DataFlow, Kistler) and stored in a computer. The sampling rate was 50 Hz.

The injection grade polystyrene (PG-33, Zhenjiang Chimei Chemical Co.) with a melt index of 7.9 g/10 min (200 °C, 5 kg) was used in this work. It was dried at 80 °C for 3 h in a vacuum oven before molding.

2.2 Methodology. As listed in Table 1, four processing parameters, including the injection stroke (S_i), compression force (F_c), compression stroke (S_c), and compression speed (V_c), were investigated in terms of their influences on the profiles of the cavity pressure and mold surface strain in this work. Three levels were selected for the F_c, S_c, and V_c. To clearly disclose the relationship between the mold surface strain and S_i, five levels were considered for S_i. The barrel temperatures were set at 185–210 °C (toward the nozzle), and the mold was kept at room temperature. Other processing parameters, including the injection speed (200 mm/s) and compression delay time (0.3 s), were kept constant. It is worthy to note that the screw-driven packing stage was not adopted during ICM in this work. So, it is expected that a more uniform cavity pressure distribution and resultant higher quality parts can be obtained via the mold compression.

Table 1 Conditions of ICM experiments and results of R^2 between cavity pressures directly measured with pressure sensor at P1 and those indirectly obtained from strain sensor in compression stage

	Parameters				
Test no.	S_i (mm)	F_c (kN)	S_c (mm)	V_c (mm/s)	R^2
1	20.0	100	2	20	0.733
2	20.2	100	2	20	0.840
3	20.4	100	2	20	0.900
4	20.6	100	2	20	0.868
5	20.8	100	2	20	0.890
6	20.2	50	2	20	0.791
7	20.2	150	2	20	0.962
8	20.2	100	1	20	0.920
9	20.2	100	3	20	0.964
10	20.2	100	2	5	0.822
11	20.2	100	2	35	0.914
Average	—	—	—	—	0.873

3 Results and Discussion

3.1 Typical Profiles of Cavity Pressure and Mold Surface Strain. Figure 2 presents the profiles of both cavity pressure and mold surface strain monitored during ICM under the processing parameters listed in Table 1. As can be seen in Figs. 2(*a*)–2(*d*), regardless of the processing conditions, the pressure profiles at a given measured position (P1 or P2) show a similar trend throughout the whole molding process. At P1, as the injection is started at approximately 0 s, the pressure increases rapidly and reaches the first peak value of a rather low level (< 5 MPa). Then the pressure drops down to zero immediately at the end of the injection stage. After a slight delay (0.3 s), during which the stage is switched over from injection to compression, the pressure suddenly increases to the second peak value, followed by the gradual reduction to a plateau. The second peak values of the pressure are much higher than the first peak values. Moreover, the plateau value of the pressure is found to increase with the injection stroke (Fig. 2(*a*)). It is interesting to find

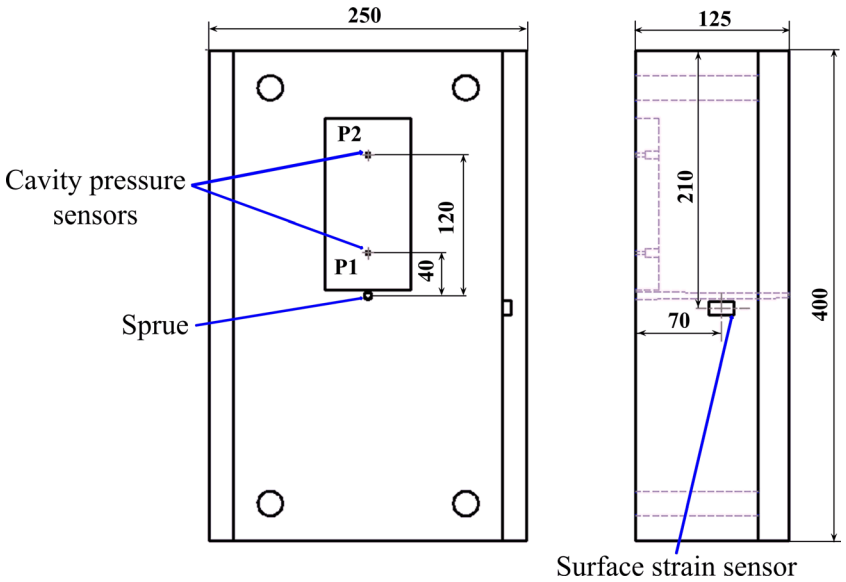

Fig. 1 Schematic of fixed mold half equipped with cavity pressure sensors and surface strain sensor (unit: mm)

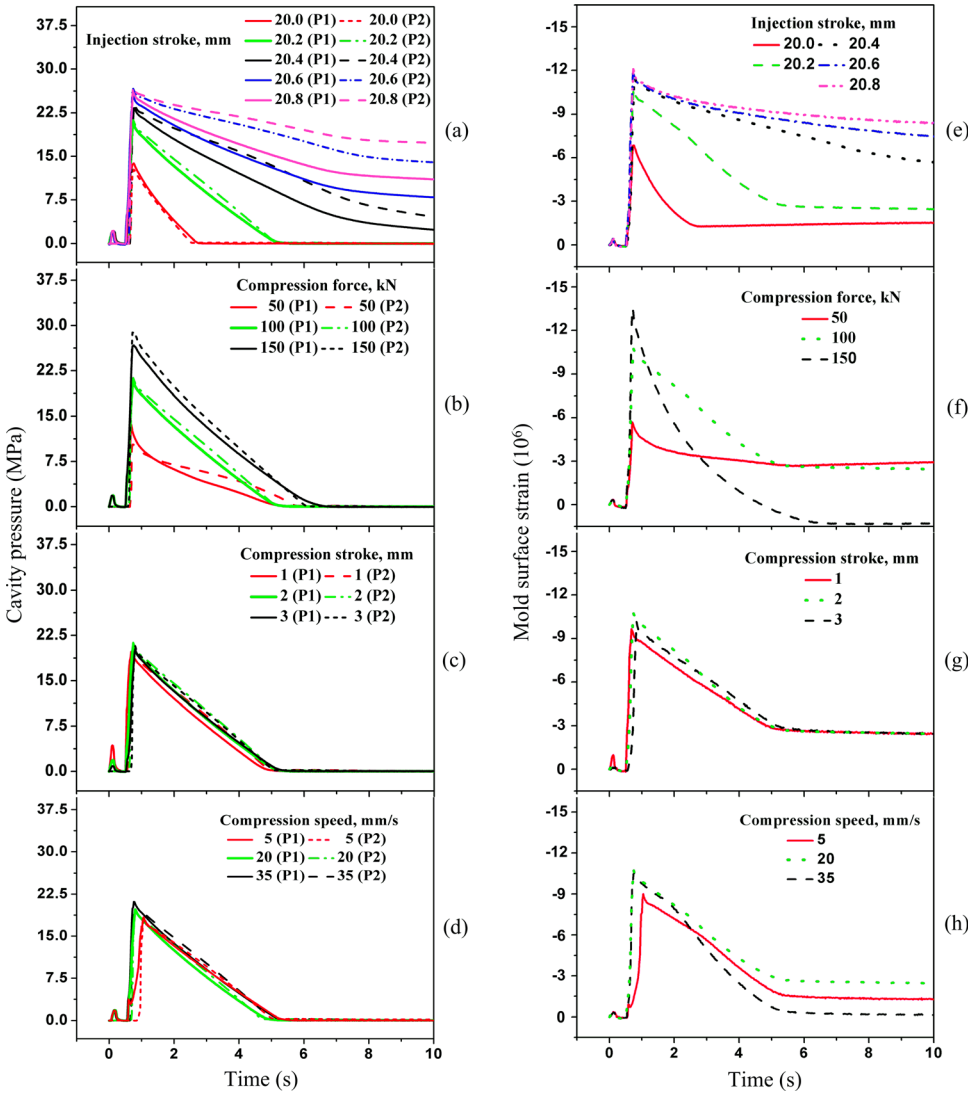

Fig. 2 Profiles of (*a*)–(*d*) cavity pressures at P1 and P2 and (*e*)–(*h*) mold surface strain during ICM under varied processing parameters

that as the mold filling is completed, a moderate cavity pressure and a more uniform cavity pressure distribution indicated by the overlapped pressure profiles at P1 and P2 can be achieved under appropriate injection strokes. This is conceivable to play a key role in producing precise parts during ICM.

It is interesting to find that the cavity pressure profile at P1 (Figs. 1(*a*)–1(*d*)) and the corresponding mold surface strain profile (Figs. 1(*e*)–1(*h*)) exhibit a remarkably similar pattern in the whole molding cycle. It is thus expected that a qualitative or even quantitative relationship between the cavity pressure and mold strain may exist during ICM. So, the mold surface strain monitoring may serve as an alternative to the direct cavity pressure monitoring in terms of providing valuable feedback for process and part quality control, and relevant analyses are presented as follows.

3.2 Quantitative Relationship Between Cavity Pressure and Mold Surface Strain. To reveal the underlying quantitative relationship between the cavity pressure and mold surface strain, the strain of the fixed mold half, where the surface strain sensor was installed (as shown in Fig. 1), was analyzed. It is suggested from Fig. 2 that rather low cavity pressure appears in the injection stage. Besides, the cavity pressure in the compression stage is crucial for the process and part quality control, and thus the focus of the current work is on this stage. In the compression stage, the mold is partly closed, and the strain of the fixed mold half results from the cavity pressure and the force transferred from the cavity plate of the moving mold half (i.e., the compression force of the springs). Detailed structure of the moving mold half can be found in Ref. [25]. Experimental results show that extremely small strain (less than 2% of the maximum strain) in the measured position of the fixed mold half results from the compression force of the springs, and so can be neglected compared with that imposed by the cavity pressure. This can be interpreted as follows: (a) the compression force of the spring is quite small; (b) the compression force of the spring acts on the positions near the edge of the mold, and thus results in the lowest strain near the middle of the mold, where the strain sensor was installed. Therefore, the mold strain is mainly ascribed to the cavity pressure. Based on the Hooke's law, it can be believed that within the elastic limit of the steel mold, the cavity pressure (P) is directly proportional to the mold surface strain (ε), i.e., $P = k \cdot \varepsilon$, where k is a scale factor. However, it is expected that, as the mold is completely closed, this relationship would not hold true anymore, due to the fact that the clamping force imposed on the cavity plate increases and yields corresponding strain on the fixed mold half.

The linear regression was carried out to determine the foregoing dependence of the P on ε. And the following equation can be applied [26].

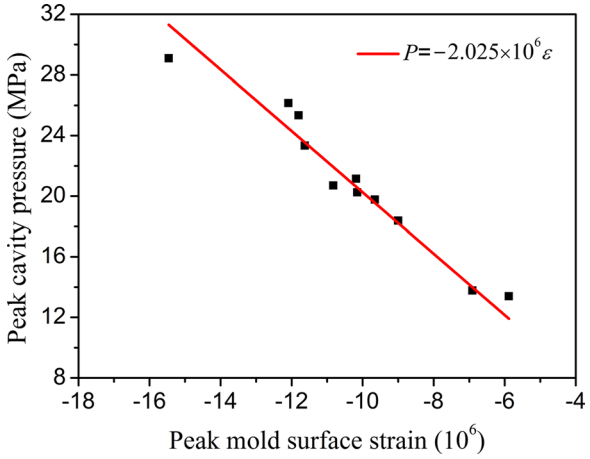

Fig. 3 Result of regression analysis for relationship between peak cavity pressure at P1 and peak mold strain monitored in compression stage

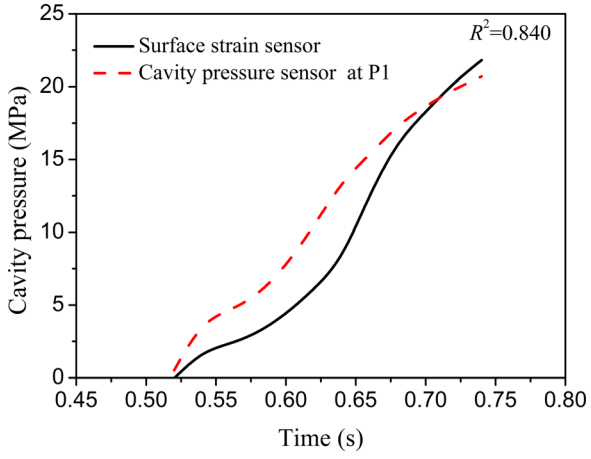

Fig. 4 Representative cavity pressure profiles directly measured at P1 and obtained from strain sensor in compression stage (test no. 2)

Table 2 ANOVA result of regression for relationship between peak cavity pressure at P1 and peak mold surface strain in compression stage

Source of variation	Degrees of freedom	Sum of squares	Mean square	F statistic
Model	1	5086.5	5087.5	3637.1
Residual	10	14.0	1.4	—
Total	11	5100.5	—	—

$$k = \sum_{i=1}^{m} P_i \varepsilon_i \Big/ \sum_{i=1}^{n} \varepsilon_i^2 \tag{1}$$

where m is the total number of tests ($m = 11$ in this work).

From Eq. (1), the correlation between the peak values of the cavity pressure and mold surface strain in the compression stage was obtained, that is, $P = -2.025 \times 10^6 \varepsilon$, where the unit for the P is MPa. And the 95% confidence interval of the k extends from -2.100×10^6 to -1.950×10^6. Such a narrow confidence interval suggests a high reliability of the calculated k value. Figure 3 represents the experimentally obtained data and linear regression model. Moreover, the significance of the coefficient k in the regression was estimated by the F-test, and the F statistic was determined using the analysis of variance [26]. The result is summarized in Table 2. It was found that the computed F statistic shows a high level of 3637.1. Given one and ten degrees of freedom (Table 2) and a 0.05 significance level, the critical F value can be obtained from the F distribution tables [26], which is 4.96. So the computed F value is overwhelmingly significant compared with critical F value, and the regression model can well describe the relationship between the peak cavity pressure and peak mold surface strain.

By applying the aforementioned function, the mold surface strain profiles were converted into the cavity pressure profiles, which were compared with the cavity pressure profiles directly measured by the pressure sensor at P1. The representative result (test no. 2) is displayed in Fig. 4. A reasonable agreement can be observed between these two pressure profiles. To quantify the degree of correlation, the analyses of determination coefficient R^2 [27] between these two kinds of curves were carried out for the results from each experiment studied.

$$R^2 = 1 - SS_{\text{err}}/SS_{\text{tot}} \tag{2}$$

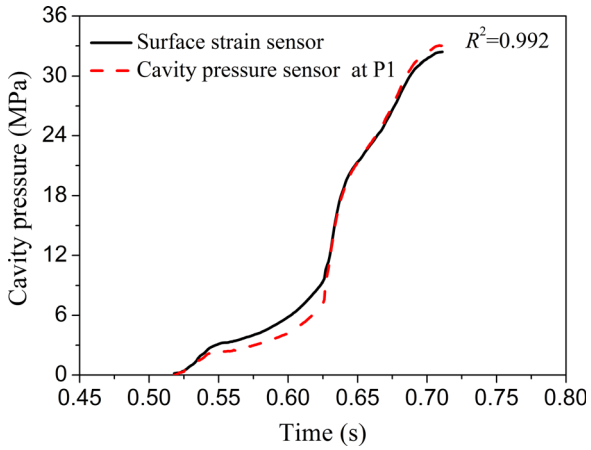

Fig. 5 Cavity pressure profiles measured with pressure sensor at P1 and obtained from strain sensor in compression stage under optimized molding conditions. Injection stroke: 20.8 mm, compression force: 150 kN, compression stroke: 3 mm, compression speed: 35 mm/s.

$$SS_{\text{err}} = \sum_{i=1}^{n} \left(P_i - \hat{P}_i\right)^2 \tag{3}$$

$$SS_{\text{tot}} = \sum_{i=1}^{n} \left(P_i - \bar{P}\right)^2 \tag{4}$$

where SS_{err} is the residual sum of squares, SS_{tot} is the total sum of squares, n is the total number of observed values, $\bar{P}$ is the average value of directly measured cavity pressures, and $\hat{P}_i$ represents indirectly obtained cavity pressure.

The results of R^2 are listed in Table 1. As can be seen, for all the experiments carried out in this work the R^2 varies from 0.733 to 0.964, and the average value of the R^2 reaches 0.873. To further improve the pressure acquisition accuracy of the proposed technique, that is, to increase the R^2 value, the optimization of the molding conditions was carried out according to the result of Table 1. As can been seen from this table, a high level of each molding parameter may ensure better accuracy of the indirect pressure measurement. To confirm this, an additional ICM experiment under the molding parameters of highest levels was carried out. The pressure profiles acquired from direct and indirect methods are displayed in Fig. 5. Interestingly, these two profiles agree

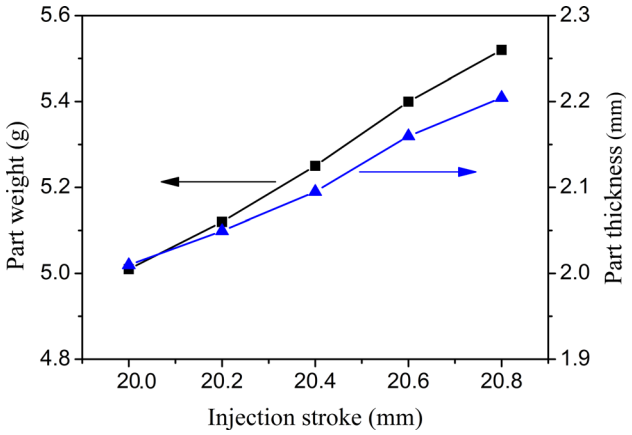

Fig. 6 Part weight and thickness under varied injection strokes. Compression force: 100 kN, compression stroke: 2 mm, compression speed: 20 mm/s.

well with each other in the compression stage. The R^2 value between them achieves 0.992, which evidences a strong correlation and the feasibility of the cavity pressure acquisition using a surface strain sensor in the compression stage of ICM. Actually, the mounting location of the surface strain sensor affects the acquisition quality and signal-to-noise ratio of obtained cavity pressure, which will be reported in a separated work elsewhere [25]. For the mounting location selected in this work (Fig. 1), the strain sensor shows a quite satisfactory performance in terms of the pressure acquisition.

3.3 Detection of Mold/Part Separation and Part Weight. As can be clearly observed in Fig. 2, under smaller values of injection strokes (20.0 and 20.2 mm) and all values of other parameters used in this work, the cavity pressures in both P1 and P2 and corresponding mold surface strain reach the final plateau values at almost the same time. The plateau pressure is 0 MPa in these conditions, which suggests that a large area of the part surface loses contact with the cavity surface at this moment. Then the cooling rate of the part starts to dramatically decrease [28]. Such critical moment, which is significant for the optimization and control of the cooling stage in the injection molding, is found to be detectable via the mold surface strain measurement.

It is noted that in the cooling stage the plateau value of the mold strain increases with the injection stroke (Fig. 2(*e*)). Under different injection strokes, the average thickness along the flow path and weight of the mold parts were measured, and the results are displayed in Fig. 6. As can be seen, an approximately linear relationship exists between the part weight or thickness and injection stroke. It is suggested from Figs. 2(*e*) and 6 that the part weight or thickness, which is widely considered to be a useful feedback for part quality monitoring and control in the injection molding, can be reflected via the plateau value of the mold surface strain. That is, the mold surface strain monitoring can serve as an alternative to the cavity pressure monitoring in terms of detecting the weight or thickness of ICM part.

4 Conclusions

In the current work, a new technique was proposed for the cavity pressure acquisition in the ICM. In an indirect and nondestructive manner, the cavity pressure in the compression stage was obtained from a strain sensor mounting on the external surface of the mold. This acquisition technique relied on a directly proportional relationship between the cavity pressure and mold surface strain, which was determined via the regression analysis. High acquisition accuracy of cavity pressure was achieved under higher levels of injection stroke, compression force, compression stroke, and compression speed. Moreover, the mold surface strain profile could reflect the part weight or thickness and the critical time when the part cooling rate started to be abruptly reduced due to the disappearance of contact between the part and cavity surfaces in a large area. The monitoring of the mold surface strain could provide valuable online feedback for the process and part quality control in ICM.

Acknowledgment

Financial support provided by the Doctoral Program of Higher Education of China (20120172110001) and Program for Changjiang Scholars and Innovative Research Team in University is gratefully acknowledged.

Nomenclature

ANOVA = analysis of variance
F_c = compression force
ICM = injection-compression molding
k = scale factor
P = cavity pressure
P1 = measured position 1
P2 = measured position 2
$\bar{P}$ = average value of directly measured cavity pressures
$\hat{P}_i$ = cavity pressure indirectly obtained with strain sensor
R^2 = coefficient of determination
S_c = compression stroke
S_i = injection stroke
SS_{err} = residual sum of squares
SS_{tot} = total sum of squares
V_c = compression speed
ε = mold surface strain

References

[1] Chen, Z. B., and Turng, L. S., 2005, "A Review of Current Developments in Process and Quality Control for Injection Molding," Adv. Polym. Technol., **24**(3), pp. 165–182.
[2] Kazmer, D. O., Velusamy, S., Westerdale, S., Johnston, S., and Gao, R. X., 2010, "A Comparison of Seven Filling to Packing Switchover Methods for Injection Molding," Polym. Eng. Sci., **50**(10), pp. 2031–2043.
[3] Yang, Y., and Gao, F. R., 1999, "Cycle-to-Cycle and Within-Cycle Adaptive Control of Nozzle Pressure During Packing-Holding for Thermoplastic Injection Molding," Polym. Eng. Sci., **39**(10), pp. 2042–2063.
[4] Woll, S. L. B., and Cooper, D. J., 1996, "Online Pattern-Based Part Quality Monitoring of the Injection Molding Process," Polym. Eng. Sci., **36**(11), pp. 1477–1488.
[5] Pramujati, B., Dubay, R., and Samaan, C., 2006, "Cavity Pressure Control During Cooling in Plastic Injection Molding," Adv. Polym. Technol., **25**(3), pp. 170–181.
[6] Huang, M. S., 2007, "Cavity Pressure Based Grey Prediction of the Filling-to-Packing Switchover Point for Injection Molding," J. Mater. Process. Technol., **183**(2–3), pp. 419–424.
[7] Kamal, M. R., Varela, A. E., and Patterson, W. I., 1999, "Control of Part Weight in Injection Molding of Amorphous Thermoplastics," Polym. Eng. Sci., **39**(5), pp. 940–952.
[8] Zeaiter, M., Knight, W., and Holland, S., 2011, "Multivariate Regression Modeling for Monitoring Quality of Injection Moulding Components Using Cavity Sensor Technology: Application to the Manufacturing of Pharmaceutical Device Components," J. Process Control, **21**(1), pp. 137–150.
[9] Griffiths, C. A., Dimov, S. S., Scholz, S., Hirshy, H., and Tosello, G., 2011, "Process Factors Influence on Cavity Pressure Behavior in Microinjection Moulding," ASME J. Manuf. Sci. Eng., **133**(3), p. 031007.
[10] Chen, S. C., Chen, Y. C., and Peng, H. S., 2000, "Simulation of Injection-Compression-Molding Process. II. Influence of Process Characteristics on Part Shrinkage," J. Appl. Polym. Sci., **75**(13), pp. 1640–1654.
[11] Chen, S. C., Chen, Y. C., Peng, H. S., and Huang, L. T., 2002, "Simulation of Injection-Compression Molding Process, Part 3: Effect of Process Conditions on Part Birefringence," Adv. Polym. Technol., **21**(3), pp. 177–187.
[12] Wu, C. H., and Chen, W. S., 2006, "Injection Molding and Injection Compression Molding of Three-Beam Grating of DVD Pickup Lens," Sens. Actuators, A, **125**(2), pp. 367–375.
[13] Michaeli, W., Hebner, S., Klaiber, F., and Forster, J., 2007, "Geometrical Accuracy and Optical Performance of Injection Moulded and Injection-Compression Moulded Plastic Parts," CIRP. Ann., **56**(1), pp. 545–548.
[14] Lee, Y. B., Kwon, T. H., and Yoon, K., 2002, "Numerical Prediction of Residual Stresses and Birefringence in Injection/Compression Molded Center-Gated Disk. Part II: Effects of Processing Conditions," Polym. Eng. Sci., **42**(11), pp. 2273–2292.

[15] Wu, C. H., and Su, Y. L., 2003, "Optimization of Wedge-Shaped Parts for Injection Molding and Injection Compression Molding," Int. Commun. Heat Mass Transfer, **30**(2), pp. 215–224.
[16] Huang, H. X., Li, K., and Li, S., 2009, "Injection-Compression Molded Part Shrinkage Uniformity Comparison Between Semicrystalline and Amorphous Plastics," Polym.-Plast. Technol. Eng., **48**(1), pp. 64–68.
[17] Guan, W. S., and Huang, H. X., 2012, "Back Melt Flow in Injection-Compression Molding: Effect on Part Thickness Distribution," Int. Commun. Heat Mass Transfer, **39**(6), pp. 792–797.
[18] Yang, C., Huang, H. X., and Li, K., 2010, "Investigation of Fiber Orientation States in Injection-Compression Molded Short-Fiber-Reinforced Thermoplastics," Polym. Compos., **31**(11), pp. 1899–1908.
[19] Hu, S. T., Chiu, H. S., Chien, C. C., Yu, C. K., and Chang, R. Y., 2010, "True 3D Numerical Simulation in Injection Compression Molding (ICM)," SPE ANTEC Tech Papers, Vol. 1, pp. 716–720.
[20] Tandeske, D., 1991, *Pressure Sensors: Selection and Application*, Marcel Dekker, New York.
[21] Grudzien, C. P., 1992, "Optical Pressure Transducer," U.S. Patent No. 5,127,269.
[22] Gao, R., Fan, Z., and Kazmer, D., 2008, "Injection Molding Process Monitoring Using a Self-Energized Dual-Parameter Sensor," CIRP Ann., **57**(1), pp. 389–393.
[23] Gao, R., and Kazmer, D., 2012, "Multivariate Sensing and Wireless Data Communication for Process Monitoring in RF-Shielded Environment," CIRP Ann., **61**(1), pp. 523–526.
[24] Whiteside, B. R., Martyn, M. T., Coates, P. D., Greenway, G., Allen, P., and Hornsby, P., 2004, "Micromoulding: Process Measurements, Product Morphology and Properties," Plast. Rubbers Compos., **33**(1), pp. 11–17.
[25] Guan, W. S., Huang, H. X., and Wu, Z., 2012, "Manipulation and Online Monitoring of Micro-Replication Quality During Injection-Compression Molding," J. Micromech. Microeng., **22**(11), p. 115003.
[26] Box, G. E. P., Hunter, W. G., and Hunter, J. S., 1978, *Statistics for Experimenters: An Introduction to Design, Data Analysis, and Model Building*, John Wiley & Sons Inc., New York.
[27] Draper, N. R., and Smith, H., 1998, *Applied Regression Analysis*, Wiley, New York.
[28] Beaumont, J. P., Nagel, R., and Sherman, R., 2002, *Successful Injection Molding: Process, Design, and Simulation*, Hanser Publications, Munich.